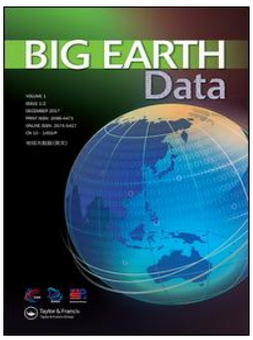

Big Earth Data

ISSN: 2096-4471 (Print) 2574-5417 (Online) Journal homepage: http://www.tandfonline.com/loi/tbed20

Atmospheric heat source/sink dataset over the Tibetan Plateau based on satellite and routine meteorological observations

Anmin Duan, Senfeng Liu, Yu Zhao, Kailun Gao & Wenting Hu

To cite this article: Anmin Duan, Senfeng Liu, Yu Zhao, Kailun Gao & Wenting Hu (2018): Atmospheric heat source/sink dataset over the Tibetan Plateau based on satellite and routine meteorological observations, Big Earth Data, DOI: 10.1080/20964471.2018.1514143

To link to this article: https://doi.org/10.1080/20964471.2018.1514143

Published online: 11 Sep 2018.

BIG EARTH DATA
https://doi.org/10.1080/20964471.2018.1514143

RESEARCH ARTICLE

OPEN ACCESS Check for updates

Atmospheric heat source/sink dataset over the Tibetan Plateau based on satellite and routine meteorological observations

Anmin Duan[a,b,c], Senfeng Liu[a,b], Yu Zhao[a,b], Kailun Gao[a,b] and Wenting Hu[a,b]

[a]State Key Laboratory of Numerical Modeling for Atmospheric Sciences and Geophysical Fluid Dynamics, Institute of Atmospheric Physics, Chinese Academy of Sciences, Beijing, China; [b]University of Chinese Academy of Sciences, Beijing, China; [c]Key Laboratory of Meteorological Disaster and Collaborative Innovation Center on Forecast and Evaluation of Meteorological Disasters, Nanjing University of Information Science & Technology, Nanjing, China

ABSTRACT

The Tibetan Plateau (TP), acting as a large elevated land surface and atmospheric heat source during spring and summer, has a substantial impact on regional and global weather and climate. To explore the multi-scale temporal variation in the thermal forcing effect of the TP, here we calculated the surface sensible heat and latent heat release based on 6-h routine observations at 80 (32) meteorological stations during the period 1979–2016 (1960–2016). Meanwhile, *in situ* air-column net radiation cooling during the period 1984–2015 was derived from satellite data. This new dataset provides continuous, robust, and the longest observational atmospheric heat source/sink data over the third pole, which will be helpful to better understand the spatial-temporal structure and multi-scale variation in TP diabatic heating and its influence on the earth's climatic system.

ARTICLE HISTORY
Received 31 May 2018
Accepted 15 August 2018

KEYWORDS
Atmospheric heat source/sink; dataset; Tibetan Plateau; sensible heat; latent heat

1. Introduction

The Tibetan Plateau (TP) plays a key role in the formation and variation in the Asia summer monsoon via its mechanical and thermal effects (An et al., 2015; Boos & Kuang, 2010; Luo & Yanai, 1984; Wu et al., 2015; Ye & Gao, 1979; Yeh, 1950; Zhao & Chen, 2001). TP thermal effects vary at different time scales and have a significant influence on surrounding circulations, particularly during spring and summer (Chen, Reiter, & Feng, 1985; Duan et al., 2012; Wu et al., 1997). In recent years, as climate change has become a research hotspot, the TP has also received more attention as the "third pole" of the Earth (Yao et al., 2012).

Due to rare observational records and inhomogeneous distribution of meteorological stations over TP, accurately estimating the intensity and change in TP thermal forcing remains a great challenge. Luo and Yanai (1984) estimated the TP atmospheric heat source in 1979 via a reverse computational method, and many following studies have created different reanalysis datasets to obtain domain-covered and long-term datasets

CONTACT Anmin Duan amduan@lasg.iap.ac.cn State Key Laboratory of Numerical Modelling for Atmospheric Sciences and Geophysical Fluid Dynamics (LASG), Institute of Atmospheric Physics (IAP), Chinese Academy of Sciences (CAS), P.O. Box 9804, Beijing 100029, China

of the TP atmospheric heat source (e.g. Qi, Li, Li, Chen, & De, 2010; Zhu, Ding, & Xu, 2007), However, the results from the different reanalysis datasets are not completely consistent, with some even showing opposite signals (Wang, Zhou, & Duan, 2012). On the basis of station observations and satellite data from the International Satellite Cloud Climatology Project (ISCCP), Duan and Wu (2008) showed a weakening trend in the TP atmospheric heat source during the period 1961–2003, particularly in the spring surface sensible heat flux since the 1980s. Yang, He, et al. (2010) argued that the effect of heat exchange and biases of the surface net radiation in satellite data and in China Meteorological Administration (CMA) gauge-measured precipitation may influence the estimated trend in the TP atmospheric heat source.

In contrast to a cooling trend in other parts of China and the hiatus of climate warming for the global mean since 1998, rapid climate warming still persists over the TP (Duan & Xiao, 2015), whereas the accompanying change in the TP atmospheric heat source remains an open question. Therefore, a reliable dataset of TP thermal forcing has become an indispensable resource for researchers. However, because of the complexity of the land surface process over the TP, most reanalysis data fail to provide an accurate measure of its statistical features let alone its multi-timescale variability. This makes station observations over the TP particularly important to estimate its thermal conditions. In fact, starting in 1960, the Chinese government has continued supporting observations over the TP under severe ecological conditions. Over time, the number of stations and the reliability of observations are constantly increasing. Compared with the study of Duan and Wu (2008), a longer and continuous dataset with more advanced parameterization scheme is required to support for research on the TP heating effect and a reliable reference for the evaluation of the quality of different reanalysis datasets.

2. Data product and generation algorithms

2.1. *Introduction of data product*

Atmospheric heat source/sink (E) is usually used as a quantitative analysis tool to calculate the heat budget in an air column. It is defined as a net heat gain (loss) existing at a given location within a given time period. Therefore, the expression of E is as follows:

$$E = SH + LH + RC \tag{1}$$

where SH represents the local sensible heat transfer at the surface, LH denotes the latent heat released to the atmosphere via precipitation, and $RC$is the net radiation flux of the air column.

Thus, the atmospheric heat source/sink dataset over the TP in this study consists of three variables: surface sensible heat flux SH, latent heat release LH and net radiation flux RC. Figure 1 shows a brief introduction of the main components and primary data sources in the dataset. According to the estimating method proposed by Yang, Qin, Guo, Zhou, and Ma (2009), air temperature at 1.5 m and surface temperature and wind speed at 10 m in CMA station observations are used to calculate surface sensible heat flux, while the latent heat release is estimated using CMA precipitation data. The locations and elevations of 80 CMA stations over the TP are shown in Figure 2. Most of the CMA stations are in the eastern-central TP. In the western TP,

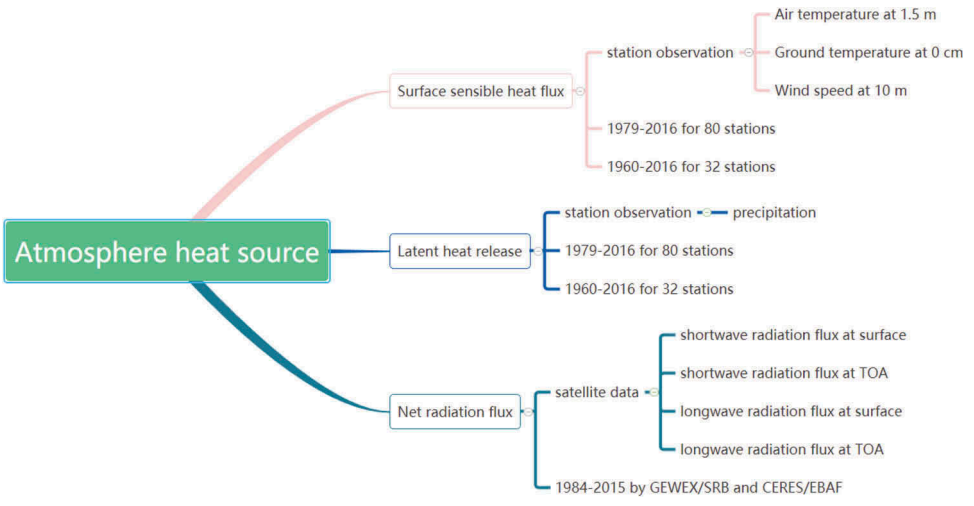

Figure 1. Diagram of dataset components and sources.

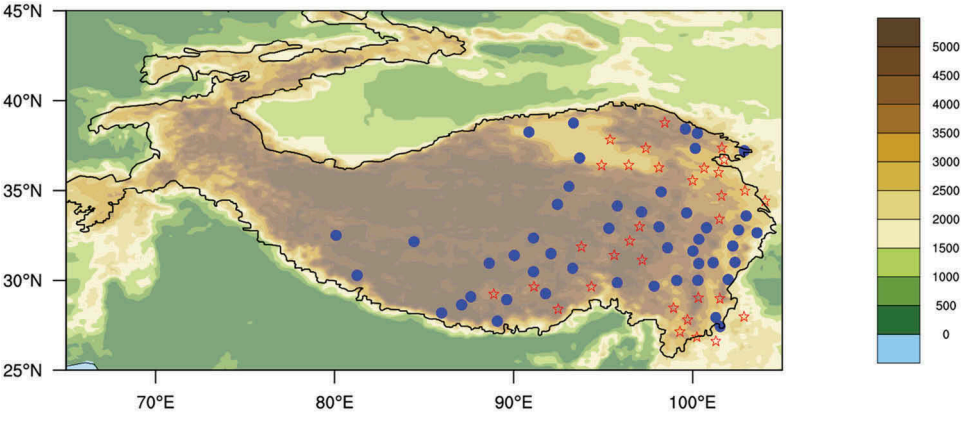

Figure 2. The distribution of 80 Chinese Meteorological Administration (CMA) stations over the TP (Pentagrams and solid circles denote 32 stations covering 1960–2016 and 48 stations covering 1979–2016, respectively.) and the color label denotes the altitude (Unit: m). The black curve outlines the TP area with an averaged altitude higher than 2000 m.

there are only three stations to the west of 85°E with an altitude higher than 4000 m. To obtain a continuous dataset of surface sensible heat flux and latent heat release as long as is possible, we classified 80 stations into two types. Because of the different times of station construction and observational interruptions, 48 out of the 80 stations own 38 years of continuous observations from January 1, 1979 to December 31, 2016 (solid circles in Figure 2; detailed information is provided in Table 1), while the other 32 stations have continuous and longer observations in a common time range that covers 57 years from January 1, 1960 to December 31, 2016 (pentagrams in Figure 2; see Table 2).

The satellite datasets used to calculate the net radiation flux were the Global Energy and Water Cycle Experiment surface radiation budget satellite radiation (GEWEX/SRB,

Table 1. Name, ID, latitude, and longitude of 48 CMA stations for the 1979–2016 timespan.

No.	Name	ID	Latitude (N)	Longitude (E)
1	Mangya	51,886	38°15′	90°51′
2	Lenghu	52,602	38°45′	93°20′
3	Yeniugou	52,645	38°25′	99°35′
4	Qilian	52,657	38°11′	100°15′
5	Xaozaoho	52,707	36°48′	93°41′
6	Gangcha	52,754	37°20′	100°08′
7	Wushaoling	52,787	37°12′	102°52′
8	Wudaoliang	52,908	35°13′	93°05′
9	Shiquanhe	55,228	32°30′	80°05′
10	Gaize	55,248	32°09′	84°25′
11	Bange	55,279	31°23′	90°01′
12	Amdo	55,294	32°21′	91°06′
13	Naqu	55,299	31°29′	92°04′
14	Bulan	55,437	30°17′	81°15′
15	Shenzha	55,472	30°57′	88°38′
16	Tangxiong	55,493	30°29′	91°06′
17	Lazi	55,569	29°05′	87°36′
18	Zedang	55,598	29°15′	91°46′
19	Nielamu	55,655	28°11′	85°58′
20	Dingri	55,664	28°38′	87°05′
21	Jiangzi	55,680	28°55′	89°36′
22	Pali	55,773	27°44′	89°05′
23	Tuotuohe	56,004	34°13′	92°26′
24	Zaduo	56,018	32°54′	95°18′
25	Qumalai	56,021	34°08′	95°47′
26	Maduo	56,033	34°55′	98°13′
27	Qingshuihe	56,034	33°48′	97°08′
28	Shiqu	56,038	32°59′	98°06′
29	Dari	56,046	33°45′	99°39′
30	Ruoergai	56,079	33°35′	102°58′
31	Dege	56,144	31°48′	98°35′
31	Ganzi	56,146	31°37′	100°00′
33	Banma	56,151	32°56′	100°45′
34	Ceda	56,152	32°17′	100°20′
35	Daofu	56,167	30°59′	101°07′
36	Markang	56,172	31°54′	102°14′
37	Hongyuan	56,173	32°48′	102°33′
38	Xiaojing	56,178	31°00′	102°21′
39	Songpan	56,182	32°39′	103°34′
40	Jiali	56,202	30°40′	93°17′
41	Pomi	56,227	29°52′	95°46′
42	Batang	56,247	30°00′	99°06′
43	Xinlong	56,251	30°56′	100°19′
44	Litang	56,257	30°00′	100°16′
45	Zuogong	56,331	29°40′	97°50′
46	Kangding	56,374	30°03′	101°58′
47	Muli	56,459	27°56′	101°16′
48	Yanyuan	56,565	27°26′	101°31′

https://eosweb.larc.nasa.gov/project/srb/srb_table) and Clouds and Earth's Radiant Energy Systems/Energy Balanced And Filled (CERES/EBAF, https://climatedataguide.ucar.edu/climate-data/ceres-ebaf-clouds-and-earths-radiant-energy-systems-ceres-energy-balanced-and-filled). The monthly shortwave and longwave radiation fluxes at the surface and at the top of the atmosphere (TOA) in GEWEX/SRB and CERES/EBAF were utilized to obtain the net radiation flux for the period 1984–2015 via statistical methods. Detailed generation algorithms of *SH*, *LH*, and *RC* are presented in the following content.

Table 2. Name, ID, latitude, and longitude of 32 CMA stations for the 1960–2016 timespan.

No.	Name	ID	Latitude (N)	Longitude (E)
1	Tuole	52,633	38°48′	98°25′
2	Dachaidan	52,713	37°51′	95°22′
3	Delingha	52,737	37°22′	97°22′
4	Menyuan	52,765	37°23′	101°37′
5	Germu	52,818	36°25′	94°54′
6	Nuomuhong	52,825	36°26′	96°25′
7	Dulan	52,836	36°18′	98°06′
8	Qiaboqia	52,856	36°16′	100°37′
9	Xining	52,866	36°43′	101°45′
10	Guide	52,868	36°02′	101°26′
11	Xinghai	52,943	35°35′	99°59′
12	Rikeze	55,578	29°15′	88°53′
13	Lhasa	55,591	29°40′	91°08′
14	Longzi	55,696	28°25′	92°28′
15	Yushu	56,029	33°01′	97°01′
16	Henan	56,065	34°44′	101°36′
17	Jiuzhi	56,067	33°26′	101°29′
18	Hezuo	56,080	35°00′	102°54′
19	Mingxian	56,093	34°26′	104°01′
20	Suoxian	56,106	31°53′	93°47′
21	Dingqing	56,116	31°25′	95°36′
22	Nangqian	56,125	32°12′	96°29′
23	Changdu	56,137	31°09′	97°10′
24	Linzhi	56,312	29°40′	94°20′
25	Daocheng	56,357	29°03′	100°18′
26	Deqin	56,444	28°29′	98°55′
27	Jiulong	56,462	29°00′	101°30′
28	Zhaojue	56,479	28°00′	102°51′
29	Zhongdian	56,543	27°50′	99°42′
30	Weixi	56,548	27°10′	99°17′
31	Lijiang	56,651	26°52′	100°13′
32	Huaping	56,664	26°38′	101°16′

The atmospheric heat source/sink dataset over the TP contains (1) daily and monthly surface sensible heat flux and latent heat release at 80 stations from January 1, 1979 to December 31, 2016; (2) daily and monthly surface sensible heat flux and latent heat release at 32 stations from January 1, 1960 to December 31, 2016; (3) monthly net radiation flux at 80 stations from January 1984 to December 2015; (4) monthly total heat source $E = SH + LH + RC$ at 80 stations from January, 1984 to December, 2015.

2.2. *Surface sensible heat flux*

Based on the Monin and Obukhov (1954)similarity theory, the surface sensible heat flux SH can be estimated with the bulk transfer equation as follows:

$$SH = \rho c_p C_H u\left(T_g - T_a\right) \tag{2}$$

where u is the wind speed at the near-surface measurement level, T_g is the ground temperature, T_a is the air temperature at the near-surface measurement level, $\rho$is the air density, c_p is the specific heat capacity at a constant pressure, and C_H is the bulk transfer coefficient for heat. When $C_H$is constant and known, Equation (2) has been widely used to calculate the surface sensible heat flux over the TP via daily data from the CMA observations to date. Although C_H has been selected as different values in previous studies (e.g. Chen et al., 1985; Duan & Wu, 2008; Feng et al., 1985; Ye & Gao, 1979; Zhao

& Chen, 2000), it is unreasonable to regard C_H as constant in a diurnal cycle. Given that C_H exhibits diurnal variation, the present study used the scheme proposed by Yang et al. (2009) to estimate the surface sensible heat flux. An iterative algorithm based on the theory of boundary layer meteorology is designed to estimate C_H empirically via the use of a high-resolution Tibetan experimental dataset. The observational CMA data for calculating Equation (1) comprise wind speed at the 10-m level (2, 08, 14, 20 BST, and 10-min maximum), ground temperature at the 0-cm level (2, 08, 14, 20 BST), air temperature at the 1.5-m level (2, 08, 14, 20 BST, daily mean, daily maximum, and daily minimum), and station pressure (2, 08, 14, 20 BST) in Beijing standard time (BST) = UTC + 8. To adapt the diurnal variations in C_H, hourly input data of wind speed, ground temperature, and air temperature are generated via using a downscaling method based on statistical relationships between the high-resolution Tibetan experimental data and the low-resolution CMA data (Yang et al., 2009).

2.3. *Latent heat release*

The latent heat release *LH* is derived from the precipitation as follows:

$$LH = P \times L_w \times \rho_w \tag{3}$$

where P is the precipitation, $L_w = 2.5 \times 10^6 J \cdot kg^{-1}$ is the condensation heat coefficient, and $\rho_w = 10^3 kg \cdot m^{-3}$ is the water density. The precipitation in Equation (3) uses the 24-h accumulated precipitation data from the CMA (20–20 BST) (Duan & Wu, 2008).

2.4. *Net radiation flux*

To produce a satellite-based radiation data with a continuous period, we choose GEWEX/SRB and CERES/EBAF which have overlapped years (2000–2007) and their time ranges are 1984–2007 for GEWEX/SRB and 2000–2015 for CERES/EBAF. These two datasets were evaluated by Pan, Liu, and Fan (2015) based on the surface observations and results showed that GEWEX/SRB produces a smaller mean bias and root mean square error (RMSE) than CERES/EBAF in China during the overlapped period. Yang, Koike, Stackhouse, Mikovitz, and Cox (2006, 2010) pointed out that GEWEX-SRB shows better performance than ISCCP-FD in estimating radiation over the TP compared with Instrumental radiation data of 11 TP stations. Thus, we choose GEWEX/SRB as the main reference for its accuracy and longer time range and try to extend the time range to 2015 with CERES/EBAF dataset. The steps to obtain the net radiation flux from these two satellite datasets are as follows. First, we performed a bilinear interpolation to interpolate monthly satellite data from a rectilinear grid to 80 stations. Then, we used the overlapping years 2000–2007 to build a linear regression model for system bias correction. In the linear regression model, we assumed the error term was normally distributed, the CERES/EBAF data at each station was supposed as the known feature x and the GEWEX/SRB data was the target value y to be predicted. The model can be described as follows:

$$y = wx + b + \varepsilon \tag{4}$$

where ε is the error term and w and b are the weight and bias to be estimated, respectively. The interpolated CERES/EBAF and GEWEX/SRB data during the period

2000–2007 were used to estimate the parameters at each station and the data after 2007 was produced using the linear model, which corrected CERES/EBAF data to GEWEX/SRB without a system mean bias. Thus, we finally obtained a dataset of 80 stations with radiation flux variables such as the shortwave radiation flux at surface/TOA (top of atmosphere), longwave radiation at surface/TOA and net radiation flux of the atmosphere column according to the following equation:

$$\mathrm{RC} = R_{\infty} - R_0 = \left(S_{\infty}^{\downarrow} - S_{\infty}^{\uparrow}\right) - \left(S_0^{\downarrow} - S_0^{\uparrow}\right) - \left(F_0^{\downarrow} - F_0^{\uparrow}\right) - F_{\infty} \tag{5}$$

where R_{∞} and R_0 are the net radiation values measured at the TOA and at the surface, respectively. Variables S and F denote shortwave and longwave radiation fluxes, respectively, where the superscripts $\downarrow$ and $\uparrow$ represent downward and upward transport of the radiation flux, respectively. More specifically, F_0 and F_{∞} denote the longwave radiation fluxes at the surface and at the TOA. From 1984 to 2007, the data relies on GEWEX/SRB only, and it is based on both GEWEX/SRB and CERES/EBAF during the period 2008–2015. As the bias has been corrected, the data can be viewed as a long continuous period.

3. Evaluation of data product

Figure 3 presents the time sequences of annual-mean *SH*, *LH*, and *RC* over the TP. The long-term trend (dashed lines in Figure 3) was calculated by simple linear regression. In terms of annual means, the 32-station averaged value of surface sensible heat *SH* is smaller than the 48-station averaged, while the latent heat release *LH* is larger (Figure 3(a,b)). This is due to the altitudes of the 48 stations are higher than that of 32 stations (Figure 2), which mainly induces the systematic differences of surface heat fluxes between the two groups. Furthermore, the *SH* and *LH* of the 32-station average have a similar decadal trend and interannual variations to that of the 48-station and 80-station averages since 1980s (Figure 3). Thus, it is reliable to

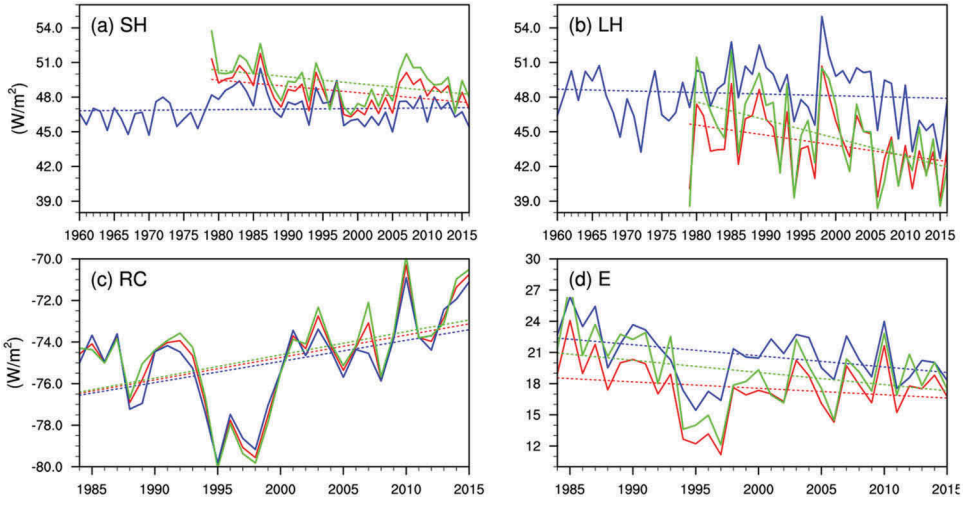

Figure 3. Temporal evolution of annual averaged (a) SH, (b) LH, (c) RC and (d) E over TP (units: W/m^2). Curves in blue are 32-station averaged, curves in green are 48-station averaged and curves in red are 80-station averaged.

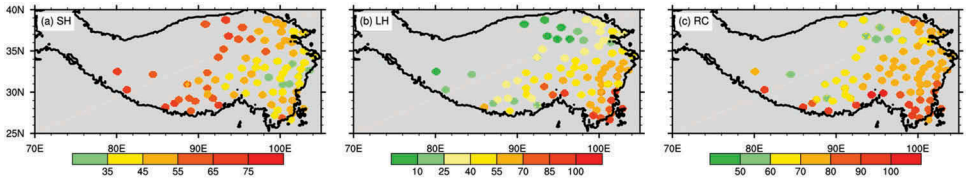

Figure 4. Spatial distribution of climatological (a) SH flux and (b) LH flux over the TP during the period 1979–2016 and (c) RC, which is multiplied by −1 to represent the radiation cooling of the atmosphere over the TP during the period 1984–2015 (units: W/m^2). The black curve outlines the TP area with an averaged altitude higher than 2500 m.

use the 32-station data from 1960 to 2016 to examine features of heat budget over the eastern TP at a longer timescale. The surface sensible heat *SH* has decreased significantly since the middle 1980s (Figure 3(a)). The latent heat release also has an obvious decreasing trend during the period 1979–2016 (Figure 3(b)), while the net radiation flux *RC* shows a significant increasing trend during the period 1984–2015 (Figure 3(c)). As a result, the atmospheric heat source *E* shows a significant decreasing trend in the period of 1984–2015 (Figure 3(d)). These results of surface heat fluxes, radiation cooling, and atmospheric heat source are consistent with the results revealed by many studies (Duan, Li, Wang, & Wu, 2011; Duan & Wu, 2008; Wang et al., 2012; Yang et al., 2009; Zhu, Liu, & Wu, 2012). Figure 4 shows the spatial distribution of the three components of atmospheric heat source/sink over the TP. The climatological fields indicate that the surface sensible heat flux *SH* is dominant in the west-central TP (Figure 4(a)), while the latent heat release *LH* and radiation cooling *RC* are largest in the south-eastern corner of the TP (Figure 4(b,c)).

This dataset benefits a further understanding of the spatial-temporal structure and multi-scale variation in the TP heat status under climate change and its influence on the earth's climatic system. Despite all the advantages, there are still some limitations and uncertainties of this new dataset. Due to the lack of CMA sites over the western TP (Figure 2), the features of atmospheric heat source in the western TP cannot be exactly described by this dataset. Moreover, it is worth noting that the surface sensible heat flux *SH* estimated by the scheme of Yang et al. (2009) only represents that from the bare-soil surfaces. Cautions must be exercised when interests are focused on the western TP and other kinds of surfaces. The next step to obtain more accurate regional atmospheric heat source over the TP area needs further include more field observations, more detailed parameterization models and consider the influence of subgrid-scale topography (Han, Ma, Chen, & Su, 2017; Ma et al., 2006, 2011).

4. Future activities

4.1. *Producing plan*

This atmospheric heat source/sink dataset over the TP will be extended in both time span and data sources every three years according to the updated status of the CMA stations and satellite datasets. The current data product was generated mainly based on GEWEX/SRB and CERES/EBAF satellite data; however, the future atmospheric heat source/sink dataset will be produced using multi-source and multi-sensor satellite data, particularly including Chinese satellite datasets.

4.2. *Contribution to CASEarth*

A project entitled "Big Earth Data Science Engineering (CASEarth)" in the Strategic Priority Research Program (SPRP) of the Chinese Academy of Sciences (CAS) was launched to collect and mine big earth data, which includes large datasets from station observations, satellites, ground sensor networks, and other sources (Guo, 2017). It will support subsequent analyses and modeling in the Earth Sciences. The third pole, i.e. the TP, is a key and typical region where the climate, terrain, and ecosystem are unique. The dataset introduced in this study will provide the longest, reliable, and continuous atmospheric heat source/sink data of the third pole, which will enrich a variety of big earth data and support the smooth implementation of CASEarth.

Data availability statement

The data that support the findings of this study are available in the personal hompage of the corresponding author, Anmin Duan, at http://www.escience.cn/people/duananmin/index.html.

Disclosure statement

No potential conflict of interest was reported by the authors.

Funding

This work was supported by the Strategic Priority Research Program of the Chinese Academy of Sciences [grant number XDA19070404] and the National Natural Science Foundation of China [grant numbers 41725018 and 91637312].

References

An, Z. S., Wu, G. X., Li, J. P., Sun, Y. B., Liu, Y. M., Zou, W. J., & Feng, J. (2015). Global monsoon dynamics and climate change. *Annual Reviews of Earth and Planet Sciences*, *43*, 29–77.

Boos, W. R., & Kuang, Z. M. (2010). Dominant control of the South Asian monsoon by orographic insulation versus plateau heating. *Nature*, *463*, 218–222.

Chen, L., Reiter, E. R., & Feng, Z. (1985). The atmospheric heat source over the Tibetan Plateau: May-August 1979. *Monthly Weather Review*, *113*, 1771–1790.

Duan, A., Li, F., Wang, M., & Wu, G. (2011). Persistent weakening trend in the spring sensible heat source over the Tibetan Plateau and its impact on the Asian summer monsoon. *Journal of Climate*, *24*(21), 5671–5682.

Duan, A. M., & Wu, G. X. (2008). Weakening trend in the atmospheric heat source over the Tibetan Plateau during recent decades. Part I: Observations. *Journal of Climate*, *21*, 3149–3164.

Duan, A. M, Wu, G. X, Liu, Y. M, Ma, Y. M, & Zhao, P. (2012). Weather and climate effects of the tibetan plateau. *Advances in Atmospheric Sciences*, *29*(5), 978–992.

Duan, A. M., & Xiao, Z. X. (2015). Does the climate warming hiatus exist over the Tibetan Plateau? *Scientific Reports*, *5*, 13711.

Feng, Z., Reiter, R. E., & Chen, L. (1985). The atmospheric heat budget over the western part of the Tibetan Plateau during MONEX. *Advances in Atmospheric Sciences*, *2*, 454–468.

Guo, H. D. (2017). Big earth data: A new frontier in earth and information sciences. *Big Earth Data*, *1*, 4–20.

Han, C., Ma, Y., Chen, X., & Su, Z. (2017). Trends of land surface heat fluxes on the Tibetan Plateau from 2001 to 2012. *International Journal of Climatology*, *37*, 4757–4767.

Luo, H. B., & Yanai, M. (1984). The large-scale circulation and heat sources over the Tibetan Plateau and surrounding areas during the early summer of 1979. Part II: Heat and moisture budgets. *Monthly Weather Review*, *112*, 966–989.

Ma, Y., Zhong, L., Su, Z., Ishikawa, H., Menenti, M., & Koike, T. (2006). Determination of regional distributions and seasonal variations of land surface heat fluxes from Landsat-7 enhanced thematic mapper data over the central Tibetan Plateau area. *Journal of Geophysics Research-Atmospheres*, *111*, D10305.

Ma, Y., Zhong, L., Wang, B., Ma, W., Chen, X., & Li, M. (2011). Determination of land surface heat fluxes over heterogeneous landscape of the Tibetan Plateau by using the MODIS and in-situ data. *Atmospheric Chemistry and Physics*, *11*, 10461–10469.

Monin, A. S., & Obukhov, A. M. (1954). Basic laws of turbulent mixing in the atmosphere near the ground. *Tr Akad Nauk SSSR Geofiz Institute*, *24*, 163–187.

Pan, X., Liu, Y., & Fan, X. (2015). Comparative assessment of satellite-retrieved surface net radiation: An examination on CERES and SRB datasets in China. *Remote Sensing*, *7*(4), 4899–4918.

Qi, D. M., Li, Y. Q., Li, Y., Chen, Y. R., & De, Q. (2010). Variation of atmospheric heat source over east of the Tibetan Plateau in summer and its influence on climate of surrounding region (in Chinese). *Journal of Arid Meteorology*, *28*, 113–120.

Wang, M., Zhou, S., & Duan, A. (2012). Trend in the atmospheric heat source over the central and eastern Tibetan Plateau during recent decades: Comparison of observations and reanalysis data. *Chinese Science Bulletin*, *57*, 548–557.

Wu, G. X., Duan, A. M., Liu, Y. M., Mao, J. Y., Ren, R. C., Bao, Q., … Hu, W. T. (2015). Tibetan Plateau climate dynamics: Recent research progress and outlook. *National Science Review*, *2*, 100–116.

Wu, G. X., Li, W. P., & Liu, H. (1997). Sensible heating-driving air pump of the Tibetan Plateau and the Asian summer monsoon. Memorial Volume of Prof, J. Z. Zhao and D. Z. Ye, Eds., Science Press, Beijing, 116–126. (In Chinese)

Yang, K., He, J., Tang, W. J., Qin, J., & Cheng, C. C. K. (2010). On downward shortwave and longwave radiations over high altitude regions: Observation and modeling in the Tibetan Plateau. *Agricultural & Forest Meteorology*, *150*, 38–46.

Yang, K., Koike, T., Stackhouse, P., Mikovitz, C., & Cox, S. J. (2006). An assessment of satellite surface radiation products for highlands with Tibet instrumental data. *Geophysical Research Letters*, *33* (22), L22403.

Yang, K., Qin, J., Guo, X., Zhou, D., & Ma, Y. (2009). Method development for estimating sensible heat flux over the Tibetan Plateau from CMA data. *Journal of Applied Meteorology and Climatology*, *48*, 2474–2486.

Yao, T. D., Thompson, L., Yang, W., Yu, W. S., Gao, Y., Guo, X. J., … Joswiak, D. (2012). Different glacier status with atmospheric circulations in Tibetan Plateau and surroundings. *Nature Climate Change*, *2*, 663–667.

Ye, D., & Gao, Y. (1979). The meteorology of the Qinghai-Xizang (Tibet) Plateau (in Chinese). *Science Press*, 278.

Yeh, T.-C. (1950). The circulation of high troposphere over China in winter of 1945–1946. *Tellus*, *2*, 173–183.

Zhao, P., & Chen, L. (2000). Study on climatic features of surface turbulent heat exchange coefficients and surface thermal forces over the Qinghai-Xizang Plateau. *Acta Mechanica Sinica*, *14*, 13–29.

Zhao, P., & Chen, L. X. (2001). Climatic features of atmospheric heat source/sink over the Qinghai-Xizang Plateau in 35 years and its relation to rainfall in China. *Science in China Series D: Earth Sciences*, *44*, 858–864.

Zhu, X. Y., Liu, Y. M., & Wu, G. X. (2012). An assessment of summer sensible heat flux on the Tibetan Plateau from eight data sets. *Sciences China Earth Sciences*, *55*, 779–786.

Zhu, Y. X., Ding, Y. H., & Xu, H. G. (2007). The decadal relationship between atmospheric heat source of winter and spring snow over Tibetan Plateau and rainfall in east China (in Chinese). *Acta Meteorologica Sinica*, *65*, 946–958.